ROYAL SOCIETY
OF CHEMISTRY

PAPER

A direct microcontact printing induced supramolecular interaction for creating shape-tunable patterned polymeric surfaces†

Meiwen Peng,‡[ab] Peng Xiao,‡[b] Youju Huang,*[b] Mujin Cai,[a] Yanshan Hou,[b] Jiaming Chen,[b] Zhenzhong Liu,[b] Zhidong Xiao*[a] and Tao Chen*[b]

Multifunctional patterned polymeric surfaces are of significant importance to numerous surface-based researches. We demonstrated that a commercial polymer of polyethylenimine (PEI) with rich amino groups can be used as a versatile ink for the direct fabrication of patterned PEI surfaces *via* a supramolecular interaction between amino groups in PEI and −OH on a silicon wafer induced by micro-contact printing (μCP). The thicknesses and shapes of the formed PEI surfaces can be finely tuned by changing the molecular weight and/or the concentration of PEI. The obtained patterned polymeric surfaces could be amplified further to grow other polymer brushes, or explored as novel surface-enhanced Raman scattering (SERS) active materials by electrostatic adsorption with negatively charged gold nanoparticles (AuNPs).

Introduction

Functional polymers with patterned surfaces have attracted tremendous interest because of the abundant functionalities of polymers and a wide range of applications including cell biology, tissue engineering, medical science, optics and electronics.[1-3] These patterned polymeric surfaces could be created *via* various strategies such as photolithography (PL),[4-6] nanoimprint lithography (NIL),[7,8] soft lithography,[9,10] and Dip-pen nanolithography (DPN).[11,12] Among these methods, as one important strategy of soft lithography, microcontact printing (μCP) is a powerful and widely-used approach to achieve the patterned polymeric surfaces with high versatility in sub-micrometer accuracy.[13-15] Husemann and co-workers[16] reported the first example of a fabricated patterned polymeric surface by polymerization amplification from self-assembled monolayers (SAMs) of initiator patterns created through μCP. There is a considerable demand for patterned complex polymeric microstructures because the properties of materials are highly dependent on the complexity

of the structures. Using a multi-step μCP of initiators, in combination with deactivation of the dormant polymer chain end and atom-transfer radical polymerization (ATRP), Zhou and co-workers[17] could achieve patterned multi-component polymer brushes of high complexity. We have developed this μCP technique to fabricate various new complex polymer brush microstructures that do not exist on the original stamp *via* the "dynamic μCP"[18] or other parameter adjustment during the μCP process.[19,20] Through covalent attachment, patterned polymeric surfaces could also be fabricated by direct μCP of polymer inks such as polyethylenimine (PEI) or various polyelectrolytes on the functional target substrates *via* a chemical reaction without further polymerization.[21,22] However, this strategy lacks the possibility to achieve a complex polymeric surface. Recently, this μCP technology has been further developed by our group[23-25] to induce the supramolecular interaction between ink molecules and OH-functionalized substrates during the μCP process.

In this article, we report an alternative simple approach that a highly branched and commercially available polymer of polyethylenimine (PEI) with rich primary and secondary amino groups could be used as the ink to fabricate the patterned polymeric surfaces directly *via* a supramolecular interaction of hydrogen bonds between amino groups with a hydroxylated functionalized silicon wafer during μCP. Due to the inherent molecular properties of polymers such as long molecular chains, high viscosity, big chain entanglement and suppressed low diffusion,[26] remarkable features of the created patterned PEI surfaces can be easily tuned into various morphologies such as the necklace grid, the stripe grid, the ring array and the

[a] *Department of Chemistry, State Key Laboratory of Agricultural Microbiology, Huazhong Agricultural University, 1 Shizishan Street, Wuhan 430070, China. E-mail: zdxiao@mail.hzau.edu.cn*

[b] *Division of Polymer and Composite Materials, Ningbo Institute of Material Technology and Engineering, Chinese Academy of Science, 1219 Zhongguan West Road, Ningbo 315201, China. E-mail: tao.chen@nimte.ac.cn, yjhuang@nimte.ac.cn*

‡ These authors contributed equally to this work.

cubic array with the use of the same stamp. The obtained patterned polymeric surfaces could be amplified to grow other polymer brushes, or be explored as novel surface-enhanced Raman scattering (SERS) active materials by electrostatic adsorption with negatively charged gold nanoparticles (AuNPs).

Experimental

Materials and sample preparation

PEI (average molecular weight, M_w = 600, 1800, 10 000) was provided by Aladdin-Reagent China (Shanghai) Co., Ltd, PDMS stamps with grid configuration were fabricated from Sylgard 184 (the ratio between components A and B was 1:10) on a silicon master. The silicon wafer was cleaned in a mixture of H_2O_2/H_2SO_4, 1:3 (v/v, "piranha solution"), at 80 °C for 2 h. Subsequently, it was rinsed with deionized water abundantly and blow-dried with N_2.

Micro-contact printing (µCP)

The PDMS stamp was inked by exposing the stamp features to an ethanol solution of PEI for 3 min and drying with nitrogen, subsequently, the stamp was brought into contact with the substrate surface for 1 min to fabricate patterned PEI films on Si substrates.

Self-initiated photografting and photopolymerization (SIPGP)

The patterned polymer brushes were synthesized following a literature procedure.[23–25] The patterned substrate surface was submerged in ∼2 mL of distilled and degassed bulk monomer (for example, styrene) and irradiated with an UV fluorescent lamp with a spectral distribution between 300 and 400 nm (intensity maximum at λ = 365 nm with a total power of ∼240 mW cm^{-2}) for the required time. Then, the substrate was extensively rinsed with different solvents (toluene, ethyl acetate, and ethanol) to remove physisorbed styrene (PS) as much as possible.

Gold nanoparticle (Au NP) deposition

The Au NPs were prepared according to our previous reports.[27,28] Briefly, 100 mL of 2.5×10^{-4} M HAuCl$_4$ solution was heated to 120 °C in an oil bath under vigorous stirring for 30 min. Subsequently, 1% sodium citrate solution (5 mL for 20 nm particles) was added to the above solution with continuous boiling. After 20 min, the color of the boiled solution changed into ruby red, indicating the formation of AuNPs in the solution. The patterned substrate surface was submerged in ∼10 mL of Au NP aqueous solution for 5 min and rinsed with deionized water twice, then dried with nitrogen.
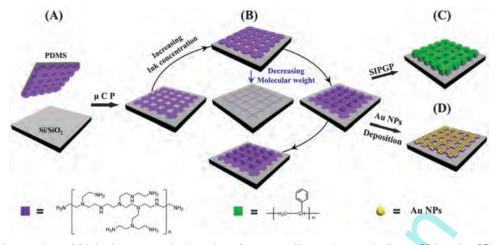
Characterization

Atomic force microscopy (AFM) images were taken using a multimode AFM (Being Nano-Instruments, Ltd) operating in the contact and/or tapping mode using silicon cantilevers (spring constant: 0.15 Nm^{-1}, resonant frequency: 12 kHz for cantilevers of contact mode, spring constant: 3–40 Nm^{-1}, resonant frequency: 75–300 kHz for cantilevers of tapping mode).

The SERS measurement is conducted on a Renishaw inVia-Reflex micro-Raman spectrometer equipped with a 633 nm laser. The Raman spectrum is calibrated using the silicon substrate. The sample is exposed to the laser for 2 s every time and is scanned 5 times under 1% total laser power.

Results and discussion

The procedure of fabricating patterned polymeric surfaces via direct µCP by using PEI as the ink molecule and their two potential applications such as further amplification of the pattern by SIPGP and interacting with AuNPs for the construction of a novel SERS active substrate are schematically shown in Scheme 1. In our present study, the silicon substrate was pretreated by "piranha solution", which endows the surface with rich –OH groups. A PDMS stamp with a grid pattern (grid size of 11 µm) was used to transfer the ink molecules onto the silicon substrate. PEI, a highly branched polymer with rich amino groups, was selected as a special ink molecule to directly fabricate the patterned polymeric surfaces via a supramolecular interaction with silicon surfaces. An ethanol solution of the PEI inked PDMS stamp, was first dried with nitrogen, and then contacted with the OH-terminated silicon substrate with a gentle force (Scheme 1A) Because the interaction of hydrogen bonds between PEI and silicon substrate interfaces is stronger than that between PDMS and PEI, micro-patterned PEI is easily transferred from the PDMS stamp onto the Si wafer once the stamp is removed after µCP. Using the same stamp, by varying the molecular weight and the concentration of PEI, various polymeric patterns such as the necklace grid, the stripe grid, the ring array and the cubic array can be easily obtained (Scheme 1B) Due to the rich amino groups of PEI, the resultant patterns can provide a plenty of photoactive sites for the further growth of polymer brushes via SIPGP (Scheme 1C). In addition, the obtained patterns can be used to fabricate novel SERS substrates by interacting with negatively charged Au NPs through electrostatic adsorption (Scheme 1D).

In order to investigate the morphology of patterned polymeric surfaces, the effects of the molecular weight and the concentration of PEI were studied. Fig. 1 shows the effect of the molecular weight of PEI on the morphology. It is obvious to see that the ink of PEI with low molecular weight (M_w = 600 or 1800) tends to form the necklace grid (Fig. 1C and D), consisting of the PEI dot array. Particularly, the size of PEI dots at each cross-point of the grid is larger than other dots, which leads to the formation of hetero-patterns. AFM images (Fig. S1A and B in the ESI†) show that PEI dots were formed on a stamp before microcontact printing because the PEI inked stamp was dewetted after drying with nitrogen.[29] The necklace grid pattern was fabricated by transferring the PEI dots on a grid stamp to a silicon wafer via µCP. As the dots at the cross-point of the grid stamp are bigger than the dots on the stripe after dewetting polymer films, a hetero-pattern was formed. The necklace grid is promising for applications such as creating large band gap photonic crystals and fleeting light.[30,31] While, under identical

8660 | J. Mater. Chem. C, 2015, 3, 8659–8664

This journal is © The Royal Society of Chemistry 2015

Scheme 1 Schematic procedure of fabricating patterned polymeric surfaces on a silicon substrate *via* direct μCP by using PEI as ink molecules (A), microstructures of a patterned PEI film are tunable by varying the ink concentration and the molecular weight (B), subsequent amplification of the patterns to grow other polymer brushes through SIPGP (C), and their use as the template for the deposition of negatively charged Au NPs (D).

experimental conditions (*i.e.*, stamp, temperature, force, and reagent concentrations) except for the use of PEI with high molecular weight (M_w = 10 000), the ink PEI likes to form a smooth and compact stripe grid polymer film on the stamp (Fig. S1C in the ESI†). After transferring to the Si substrate by μCP, a grid PEI film with a thickness over 100 nm was fabricated (Fig. 1E).

Besides molecular weight, the concentration of the ink is another critical factor to affect the morphology and the thickness of the pattern during μCP. A thin PEI pattern was achieved with a thickness below 10 nm by using a PEI ethanol solution with a concentration of 0.5 mg mL^{-1} as the ink (Fig. 2A). The thickness of the PEI patterns can be precisely controlled by varying the ink concentration. When the ink concentration increases to 2, 5, 7 and 10 mg mL^{-1}, the height of the patterns increases to 35, 52, 73 and 112 nm, respectively (Fig. 2B–E). Height of PEI films *versus* ink concentration is accompanied by a linear fitting (Fig. 2F). The AFM images of Fig. 2C and D show

Fig. 2 Tapping mode AFM height images (90 μm × 90 μm) of the PEI pattern at the ink concentration of (A) 0.5 mg mL^{-1}, (B) 2 mg mL^{-1}, (C) 5 mg mL^{-1}, (D) 7 mg mL^{-1}, and (E) 10 mg mL^{-1}. (F) Height of PEI films *versus* ink concentration accompanied by linear fitting. The M_w of PEI is 10 000.

that, with the increase of the ink concentration, the grid pattern transforms from granular into a smooth structure. The patterned polymer films with various thickness and surface roughness values are very potential in many surface-based technologies such as protein-resistant coatings, sensors, and substrates for cell-growth control.

There is a considerable demand for patterned complex polymeric microstructures because the properties of materials are highly dependent on the complexity of the structures. Our previous work reported a series of patterning strategies to obtain new complex polymer brush microstructures that do not exist on the original stamp under various μCP conditions including physical deformation, UV-ozone treatment induced chemical modification of PDMS stamp features,[19] or dynamic printing by moving or jumping the stamp during μCP,[18] in combination with surface-initiated atom-transfer radical polymerization (SI-ATRP) of *N*-isopropylacrylamide (NIPAAM). The "one stamp for shape-tunable patterns" concept is developed in direct μCP. Using the same stamp, by increasing the concentration of PEI with high molecular weight, new complex patterned
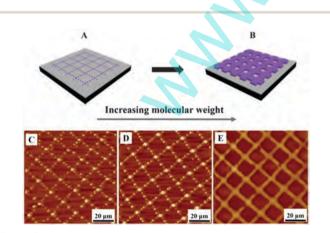

Fig. 1 Schematic illustration showing the morphology transition from a necklace grid (A) to a smooth and compact grid (B). Tapping mode AFM height images (90 μm × 90 μm) of the PEI patterns with an average M_w of (C) 600, (D) 1800 and (E) 10 000. The concentration of the PEI ink is 10 mg mL^{-1}. All the printing used the same grid PDMS stamp.
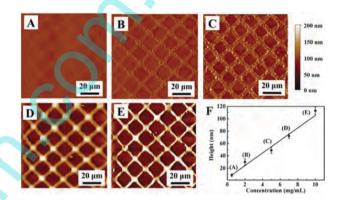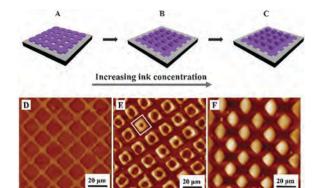
Fig. 3 Schematic illustration and the corresponding tapping mode AFM height images (90 μm × 90 μm) of three different microstructures of the patterned PEI film fabricated *via* μCP by varying the ink PEI concentration. (A and D) The grid PEI pattern on a Si wafer replicating the inked grid feature on the PDMS stamp at an ink concentration of 10 mg mL^{-1}. (B and E) When the ink concentration is increased to 20 mg mL^{-1}, the ring arrays appeared at the grid center as the PEI adhered to the wall of the groove of the inked PDMS stamp is transferred to the Si substrate. (C and F) Inverted PEI cubic arrays formed due to the concomitant transfer of inked PEI on the grid and the groove of the PDMS stamp at an ink concentration of 30 mg mL^{-1}. The M_w of the PEI is 10 000.

Fig. 4 Tapping mode AFM height images (90 μm × 90 μm) and the corresponding cross-sectional profiles of before (A and C) and after (B and D) SIPGP of the grid PEI pattern.

polymeric microstructures were achieved *via* normal μCP (Fig. 3). The stripe grid (Fig. 3A), ring array (Fig. 3B) and cubic array (Fig. 3C) PEI patterns with the same size of ∼11 μm and an enhancement of height were obtained *via* μCP by increasing the ink PEI concentration. Fig. 3D shows an AFM height image of a smooth grid pattern with ∼112 nm height and ∼11 μm distance between the stripes of the grid at the ink concentration of 10 mg mL^{-1}. That is a normal result as the size of the pattern is consistent with the features on the stamp. Upon increasing the ink concentration to 20 mg mL^{-1}, PEI ring arrays with a size of ∼11 μm and a height of ∼388 nm were fabricated, which do not exist on the original stamp (Fig. 3E). The size of the rings is ∼11 μm, corresponding to the distance between the grid. It is worth noting that the ring marked with a white pane is close to a cube structure due to the local high concentration. Fig. 3F shows cubic arrays with a size of ∼11 μm and a height of ∼503 nm at an ink concentration of 30 mg mL^{-1}. Because of the high ink concentration, inked PEI on the grid and the groove of the stamp is demolded easily from the stamp, forming an inverted PEI cubic array pattern. Due to the inherent molecular properties of the polymer such as long molecular chain, big chain entanglement, *etc.*, compact polymer bulks can be easily formed on the grid and the groove of the PDMS stamp. When the polymer bulks on the groove are small and cannot contact the substrate, the smooth and compact grid was fabricated after μCP. Upon increasing the ink concentration, polymer bulks on the groove wall were contacted and transferred to the substrate to form the ring array. The central area and the naked silicon wafer have the same height (Fig. S2, ESI†), indicating that there are no polymer films in the center of rings. Cubic arrays were formed when the polymer bulks on the grid and the groove of the stamp transferred together to substrates at a higher ink concentration.
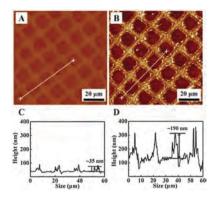
The patterns on substrates are regular because of the high viscosity and the suppressed low diffusion of the polymer. This approach provides a new way to fabricate complex patterned functional polymeric surfaces that only need one step printing by adjusting the concentration of the polymer ink.

With the development of UV polymerization, SIPGP provided us with a convenient strategy to prepare polymer brushes even without a surface bound initiator on patterned self-assembled monolayers (SAMs).[25,32] The photoactive group of primary and secondary amine groups on patterned PEI could be initiated to grow polymer brushes by SIPGP upon being immersed in various monomer solutions and irradiated with an UV lamp. The height variation of the patterned substrate surface before and after irradiation for two hours was investigated by AFM. The height of the PEI grid generated from 2 mg mL^{-1} PEI ethanol solution was about 35 nm (Fig. 4A and C). Upon employing the SIPGP, a patterned PEI-*g*-PS polymer brush with a height of ∼190 nm was formed (Fig. 4B and D).

Hammond and co-workers[33] obtained 2D arrays of particles on patterned polyelectrolyte surfaces as functional templates. In our previous work[34] we achieved stimulus-responsive, "egg-cup" shaped polymer brush microstructures on thiol initiator modified gold surfaces by μCP, which can be used as motor arrays to manipulate the movement of gold NP aggregates. Because of the patterned polyelectrolyte surface, the PEI surfaces were further used to pattern Au NPs by the electrostatic interaction between PEI and negatively charged Au NPs with a diameter of 20 nm. The morphology and the height change were investigated by AFM (Fig. 5A and B). After submerging in 10 mL of Au NP aqueous solution for 5 min, the height of the PEI pattern increased from 7 nm to 22 nm, indicating a monolayer of Au NPs adsorbed onto the patterned PEI surface (Fig. 5D). The SERS spectra of R6G based on a Si substrate exhibit a relatively weak Raman signal. Using the patterned Au NP surface as the SERS substrate, a dramatic increase in Raman signals can be observed (Fig. 5E). Bands at 614 and 774 cm^{-1} arose from the C–C–C ring in-plane and out of-plane bending vibrations, respectively. Bands at 1127 and 1185 cm^{-1} were assigned to the C–H in-plane bending and the band at 1310 cm^{-1} was assigned to the C–O–C stretching. Bands at 1361, 1511, 1572

8662 | *J. Mater. Chem. C*, 2015, **3**, 8659–8664
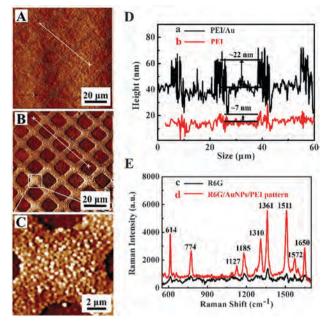
This journal is © The Royal Society of Chemistry 2015

Fig. 5 Tapping mode AFM height images before (A) and after (B and C) deposition of Au NPs. The corresponding cross-sectional profiles (D) of the PEI pattern before (b) and after (a) deposition of Au NPs. SERS spectra (E) of R6G molecules (10^{-6} M) collected on a Si substrate (c) and a patterned PEI–Au NP substrate (d).

and 1650 cm^{-1} were attributed to the C–C stretching of aromatic rings.[35] Quantitative SERS data can be estimated according to our previous work.[36] The absolute value of the enhancement factor (EF) was calculated by using the formula: EF = ISERS/IO × NO/NSERS, where ISERS and NSERS are the intensities of the band and the number of adsorbed molecules for SERS, respectively. IO and NO are the intensity of the band and the number of molecules of free R6G molecules. The intensity of Raman peaks was enhanced by an EF of approximately 6.4×10^4 for the AuNPs/PEI pattern. Such a high enhancement factor is considered to be due to the hotspot in the AuNPs/PEI pattern.

Conclusions

Based on the considerable demand to fabricate patterned complex polymeric microstructures simply, we developed the microcontact printing technology to achieve this goal using the commercially available polymer of PEI as the ink. Rich amino groups inside the branched PEI ink allow the supramolecular interaction of hydrogen bonding between PEI and the OH-functionalized silica substrate during the μCP process. Differing from the conventional "one stamp for one-shaped pattern" in direct μCP, the complex PEI morphology could be achieved to demonstrate the concept of "one stamp for shape-tunable patterns". The thicknesses and shapes of the formed PEI surfaces can be finely tuned by changing the molecular weight and the concentration of PEI. The obtained patterned polymeric surfaces could be amplified to grow other functionalized polymer brushes or explored as novel surface-enhanced Raman scattering (SERS) active materials by electrostatic adsorption with negatively charged gold nanoparticles (AuNPs).

Notes and references

1 Z. H. Nie and E. Kumacheva, *Nat. Mater.*, 2008, **7**, 277–290.
2 L. J. Xue and Y. C. Han, *Prog. Polym. Sci.*, 2011, **36**, 269–293.
3 T. Chen, I. Amin and R. Jordan, *Chem. Soc. Rev.*, 2012, **41**, 3280–3296.
4 M. S. Hahn, L. J. Taite, J. J. Moon, M. C. Rowland, K. A. Ruffino and J. L. West, *Biomaterials*, 2006, **27**, 2519–2524.
5 D. Falconnet, G. Csucs, H. M. Grandin and M. Textor, *Biomaterials*, 2006, **27**, 3044–3063.
6 E. W. H. Jager, E. Smela and O. Inganas, *Science*, 2000, **290**, 1540–1545.
7 L. J. Guo, *Adv. Mater.*, 2007, **19**, 495–513.
8 S. H. Ahn and L. J. Guo, *ACS Nano*, 2009, **3**, 2304–2310.
9 Y. N. Xia and G. M. Whitesides, *Annu. Rev. Mater. Sci.*, 1998, **28**, 153–184.
10 D. Qin, Y. N. Xia and G. M. Whitesides, *Nat. Protoc.*, 2010, **5**, 491–502.
11 R. D. Piner, J. Zhu, F. Xu, S. H. Hong and C. A. Mirkin, *Science*, 1999, **283**, 661–663.
12 X. G. Liu, S. W. Guo and C. A. Mirkin, *Angew. Chem., Int. Ed.*, 2003, **42**, 4785–4789.
13 A. Perl, D. N. Reinhoudt and J. Huskens, *Adv. Mater.*, 2009, **21**, 2257–2268.
14 R. S. Kane, S. Takayama, E. Ostuni, D. E. Ingber and G. M. Whitesides, *Biomaterials*, 1999, **20**, 2363–2376.
15 R. K. Smith, P. A. Lewis and P. S. Weiss, *Prog. Surf. Sci.*, 2004, **75**, 1–68.
16 M. Husemann, D. Mecerreyes, C. J. Hawker, J. L. Hedrick, R. Shah and N. L. Abbott, *Angew. Chem., Int. Ed.*, 1999, **38**, 647–649.
17 F. Zhou, Z. Zheng, B. Yu, W. Liu and W. T. S. Huck, *J. Am. Chem. Soc.*, 2006, **128**, 16253–16258.
18 T. Chen, R. Jordan and S. Zauscher, *Small*, 2011, **7**, 2148–2152.
19 T. Chen, R. Jordan and S. Zauscher, *Polymer*, 2011, **52**, 2461–2467.
20 T. Chen, J. Zhang, D. P. Chang, A. Garcia and S. Zauscher, *Adv. Mater.*, 2009, **21**, 1825–1829.
21 L. Yan, W. T. S. Huck, X. M. Zhao and G. M. Whitesides, *Langmuir*, 1999, **15**, 1208–1214.
22 Z. Wang, P. Zhang, B. Kirkland, Y. Liu and J. Guan, *Soft Matter*, 2012, **8**, 7630.
23 P. Xiao, J. Gu, J. Chen, D. Han, J. Zhang, H. Cao, R. Xing, Y. Han, W. Wang and T. Chen, *Chem. Commun.*, 2013, **49**, 11167–11169.

24 P. Xiao, J. Gu, J. Chen, J. Zhang, R. Xing, Y. Han, J. Fu, W. Wang and T. Chen, *Chem. Commun.*, 2014, **50**, 7103–7106.

25 P. Xiao, C. Wan, J. Gu, Z. Liu, Y. Men, Y. Huang, J. Zhang, L. Zhu and T. Chen, *Adv. Funct. Mater.*, 2015, **25**, 2428–2435.

26 T. Kaufmann and B. J. Ravoo, *Polym. Chem.*, 2010, **1**, 371.

27 Y. Huang and D.-H. Kim, *Langmuir*, 2011, **27**, 13861–13867.

28 L. Zhang, L. W. Dai, Y. Rong, Z. Z. Liu, D. Y. Tong, Y. J. Huang and T. Chen, *Langmuir*, 2015, **31**, 1164–1171.

29 C. V. Thompson, *Annu. Rev. Mater. Res.*, 2012, **42**, 399–434.

30 B. S. Song, S. Noda and T. Asano, *Science*, 2003, **300**, 1537.

31 P. Q. Zhang, X. S. Xie, Y. F. Guan, J. Y. Zhou, K. S. Wong and L. Yan, *Appl. Phys. B: Lasers Opt.*, 2011, **104**, 113–116.

32 M. Steenackers, A. Kuller, S. Stoycheva, M. Grunze and R. Jordan, *Langmuir*, 2009, **25**, 2225–2231.

33 I. Lee, H. P. Zheng, M. F. Rubner and P. T. Hammond, *Adv. Mater.*, 2002, **14**, 572–577.

34 T. Chen, D. P. Chang, J. M. Zhang, R. Jordan and S. Zauscher, *Adv. Funct. Mater.*, 2012, **22**, 429–434.

35 S. Kundu, *J. Mater. Chem. C*, 2013, **1**, 831–842.

36 Y. Huang, A. Dandapat and D.-H. Kim, *Nanoscale*, 2014, **6**, 6478–6481.